

Instantaneous spatial light interference microscopy

Huafeng Ding and Gabriel Popescu*

Quantitative Light Imaging Laboratory, Department of Electrical and Computer Engineering, Beckman Institute for Advanced Science and Technology, University of Illinois at Urbana-Champaign, Urbana, IL 61801, U.S.A.

**gpopescu@illinois.edu*

Abstract: We present Instantaneous Spatial Light Interference Microscopy (iSLIM) as a new quantitative phase method that combines the benefits of white light illumination in Zernike's phase contrast microscopy and phase stability associated diffraction phase microscopy. iSLIM is implemented as an add-on module to a commercial phase contrast microscope, and enables new features to quantitative phase imaging: diminished speckle effects due to white light illumination, multimodal investigation potential due to overlaying with other modalities of the microscope (e.g. fluorescence, DIC, phase contrast), and spectroscopic potential due to the broad band light. We show proof of principle results by multicolor phase imaging of microsphere and red blood cells, and dynamic imaging of nanoscale cell membrane fluctuations.

©2010 Optical Society of America

OCIS codes: (170.3880) Medical and biological imaging; (180.3170) Interference microscopy; (999.9999) Quantitative Phase Imaging;

References and links

1. G. Popescu, "Quantitative Phase Imaging of Nanoscale Cell Structure and Dynamics," Chap. 5 in *Methods in Nano Cell Biology* (Elsevier, 2008).
2. D. Paganin, and K. A. Nugent, "Noninterferometric phase imaging with partially coherent light," *Phys. Rev. Lett.* **80**(12), 2586–2589 (1998).
3. D. Zicha, and G. A. Dunn, "An Image-Processing System For Cell Behavior Studies In Subconfluent Cultures," *J. Microsc.* **179**, 11–21 (1995).
4. C. H. Yang, A. Wax, R. R. Dasari, and M. S. Feld, "Phase-dispersion optical tomography," *Opt. Lett.* **26**(10), 686–688 (2001).
5. M. A. Choma, A. K. Ellerbee, C. H. Yang, T. L. Creazzo, and J. A. Izatt, "Spectral-domain phase microscopy," *Opt. Lett.* **30**(10), 1162–1164 (2005).
6. C. Fang-Yen, S. Oh, Y. Park, W. Choi, S. Song, H. S. Seung, R. R. Dasari, and M. S. Feld, "Imaging voltage-dependent cell motions with heterodyne Mach-Zehnder phase microscopy," *Opt. Lett.* **32**(11), 1572–1574 (2007).
7. C. Joo, T. Akkin, B. Cense, B. H. Park, and J. F. de Boer, "Spectral-domain optical coherence phase microscopy for quantitative phase-contrast imaging," *Opt. Lett.* **30**(16), 2131–2133 (2005).
8. W. S. Rockward, A. L. Thomas, B. Zhao, and C. A. Dimarzio, "Quantitative phase measurements using optical quadrature microscopy," *Appl. Opt.* **47**(10), 1684–1696 (2008).
9. G. Popescu, T. Ikeda, R. R. Dasari, and M. S. Feld, "Diffraction phase microscopy for quantifying cell structure and dynamics," *Opt. Lett.* **31**(6), 775–777 (2006).
10. T. Ikeda, G. Popescu, R. R. Dasari, and M. S. Feld, "Hilbert phase microscopy for investigating fast dynamics in transparent systems," *Opt. Lett.* **30**(10), 1165–1167 (2005).
11. G. Popescu, L. P. Deflores, J. C. Vaughan, K. Badizadegan, H. Iwai, R. R. Dasari, and M. S. Feld, "Fourier phase microscopy for investigation of biological structures and dynamics," *Opt. Lett.* **29**(21), 2503–2505 (2004).
12. H. Ding, Z. Wang, F. Nguyen, S. A. Boppart, and G. Popescu, "Fourier transform light scattering of inhomogeneous and dynamic structures," *Phys. Rev. Lett.* **101**(23), 238102 (2008).
13. G. Popescu, Y. Park, N. Lue, C. Best-Popescu, L. Deflores, R. R. Dasari, M. S. Feld, and K. Badizadegan, "Optical imaging of cell mass and growth dynamics," *Am. J. Physiol. Cell Physiol.* **295**(2), C538–C544 (2008).
14. B. Rappaz, P. Marquet, E. Cuche, Y. Emery, C. Depeursinge, and P. J. Magistretti, "Measurement of the integral refractive index and dynamic cell morphometry of living cells with digital holographic microscopy," *Opt. Express* **13**(23), 9361–9373 (2005).
15. N. Lue, G. Popescu, T. Ikeda, R. R. Dasari, K. Badizadegan, and M. S. Feld, "Live cell refractometry using microfluidic devices," *Opt. Lett.* **31**(18), 2759–2761 (2006).

16. H. Ding, F. Nguyen, S. A. Boppart, and G. Popescu, "Optical properties of tissues quantified by Fourier-transform light scattering," *Opt. Lett.* **34**(9), 1372–1374 (2009).
 17. F. Charrière, A. Marian, F. Montfort, J. Kuehn, T. Colomb, E. Cuche, P. Marquet, and C. Depeursinge, "Cell refractive index tomography by digital holographic microscopy," *Opt. Lett.* **31**(2), 178–180 (2006).
 18. W. Choi, C. Fang-Yen, K. Badizadegan, S. Oh, N. Lue, R. R. Dasari, and M. S. Feld, "Tomographic phase microscopy," *Nat. Methods* **4**(9), 717–719 (2007).
 19. Z. Wang, L. J. Millet, M. U. Gillette, and G. Popescu, "Jones phase microscopy of transparent and anisotropic samples," *Opt. Lett.* **33**(11), 1270–1272 (2008).
 20. E. Wolf, "Solution of the phase problem in the theory of structure determination of crystals from x-ray diffraction experiments," *Phys. Rev. Lett.* **103**(7), 075501 (2009).
 21. G. Popescu, T. Ikeda, K. Goda, C. A. Best-Popescu, M. Laposata, S. Manley, R. R. Dasari, K. Badizadegan, and M. S. Feld, "Optical measurement of cell membrane tension," *Phys. Rev. Lett.* **97**(21), 218101 (2006).
 22. Y. K. Park, M. Diez-Silva, G. Popescu, G. Lykotrafitis, W. Choi, M. S. Feld, and S. Suresh, "Refractive index maps and membrane dynamics of human red blood cells parasitized by *Plasmodium falciparum*," *Proc. Natl. Acad. Sci. U.S.A.* **105**(37), 13730–13735 (2008).
 23. A. Provan, *Oxford handbook of clinical haematology* (Oxford University Press, Oxford; New York, 2004).
 24. M. Mir, Z. Wang, K. Tangella, and G. Popescu, "Diffraction Phase Cytometry: blood on a CD-ROM," *Opt. Express* **17**(4), 2579–2585 (2009).
 25. M. Mir, M. Ding, Z. Wang, K. Tangella, and G. Popescu, "Blood screening using diffraction phase cytometry," *Opt. Express* (under review).
-

1. Introduction and motivation

Quantitative Phase Imaging (QPI), i.e. mapping the phase distribution of an image field, has become a rapidly emerging area of study (for a recent review, see Ref [1]). Thus, recently various experimental approaches have been proposed [2–11]. Significantly, the knowledge of the complex (i.e. phase and amplitude) optical field across the image plane allows for numerically propagating the field in the far zone and retrieving ultrasensitive *scattering* measurements. This approach is referred to as *Fourier transform light scattering*, as it is the *spatial* analogue to Fourier transform spectroscopy [12]. The range of QPI applications in biology includes red blood cell imaging [2–4], cell growth [3,13], cell refractive index [14,15], and optical properties of tissues [16]. Recent efforts have extended this *label-free* imaging method to cell tomography [17,18], polarization imaging [19], and ultrasensitive light scattering measurements [12], which can potentially find broad applications in biomedicine.

In addition to the *resolution* and *contrast* that characterize typical, intensity-based microscopes, *phase sensitivity* is essential for the performance of a quantitative phase microscope. Diffraction Phase Microscopy (DPM) is a common-path interferometric method that was developed to provide highly stable phase measurements without degrading the diffraction limited resolution [9]. However, due to the speckle generated by the high temporal coherence light typically employed in QPI (including DPM), the contrast (or, more accurately, *contrast to noise ratio*) has not matched that achieved by white light techniques, e.g. phase contrast microscopy (PCM). Here we present Instantaneous Spatial Light Interference Microscopy (iSLIM) as a new method that combines the benefits of stability associated with DPM and that of white light illumination specific to PCM. This novel method has significant benefits compared to existing approaches, such as lack of speckles due to white light illumination, add-on capability to a commercial phase contrast microscope, multimodal investigation potential due to overlaying with other modalities of the microscope, spectroscopic potential due to the broad band light, and high stability insured by the common path geometry.

2. iSLIM principle of operation

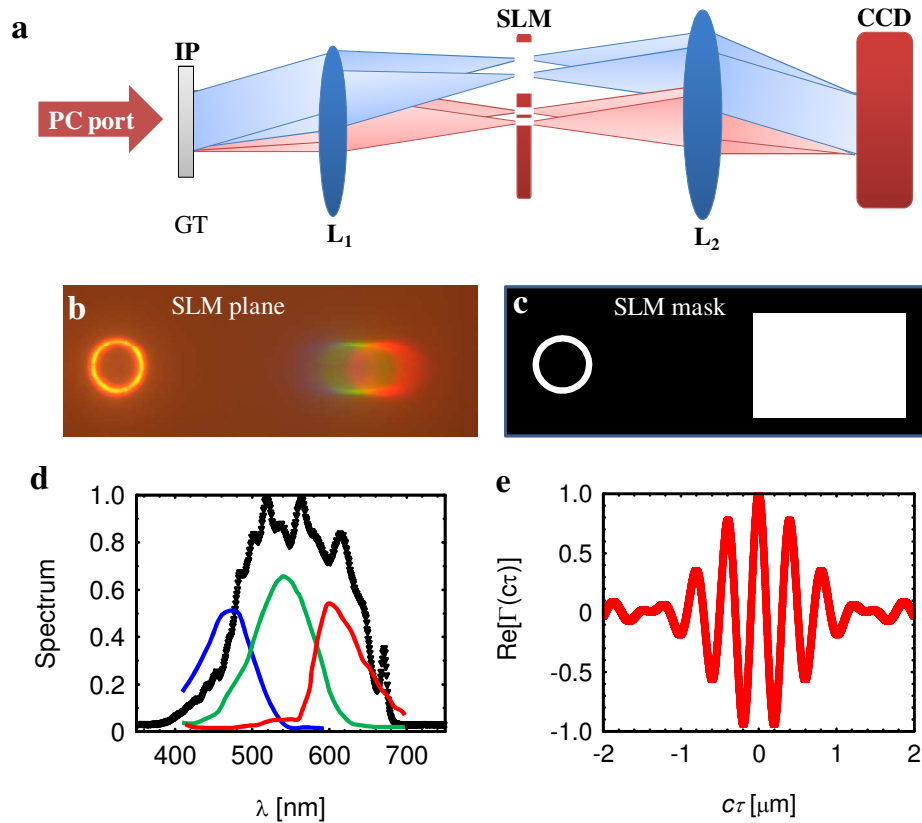


Fig. 1. a) iSLIM experimental setup: IP, image plane outputted at the phase contrast (PC) port; GT, grating; L1-L2 lenses; SLM, spatial light modulator; CCD, charged coupled device (gray scale or color). b) Intensity distribution at the SLM plane imaged by color camera. c) SLM transmission mask: white represents maximum transmission and black minimum. d) Spectrum of halogen lamp (black symbols) and spectral sensitivity for each of the red, green, and blue channels of the RGB camera. e) The temporal autocorrelation function of the illumination field; τ is the temporal delay and c the speed of light in water.

iSLIM is implemented as an add-on module to a commercial *phase contrast microscope*, which is consequently transformed into a *quantitative phase microscope*. As shown in Fig. 1(a), iSLIM employs spatially coherent white light illumination, commonly obtained from a halogen lamp and spatially filtered through the condenser annulus of the PCM (Axio Observer Z1, Zeiss). With this modification, the common path geometry specific to DPM provides not only high phase sensitivity and diffraction limited transverse resolution, but also high contrast to noise. Like in DPM [9], at the image plane (IP) of the inverted microscope, we place an amplitude diffraction grating, which generates distinct diffraction orders. We separate these orders in the Fourier plane generated by lens 1, where only the 0th and 1st orders are allowed to pass. Figure 1(b) shows this Fourier plane as imaged by a color camera, where the 1st diffraction order shows the color spread due to the grating dispersion. Note that the lens system L1-L2 forms a highly stable Mach-Zehnder interferometer. In order to generate the reference beam for this interferometer, the 0th order is spatially low-passed filtered by the spatial light modulator (SLM). The SLM filter is designed to match identically the actual image of the condenser annulus, such that only the DC component of the 0th order is passed, as shown in Fig. 1(c). Finally, at the CCD plane, we obtain an interferogram that

has high-contrast due to the intrinsic coherence matching and comparable power levels of the two beams, and is extremely stable due to the common path geometry. The spectrum of the illumination field is shown in Fig. 1(d). Using the Wiener-Kintchin theorem, which establishes the Fourier relationship between the power spectrum and autocorrelation function, we obtained the temporal correlation function Γ , the real part of which is shown in Fig. 1(e). Note that because of the full spatial coherence, Γ is expected to factorize into amplitude and phase term,

$$\Gamma(\tau) = |\Gamma(\tau)| e^{i\omega_0\tau} \quad (1)$$

This factorization is evident from the measurement of Γ , as shown in Fig. 1(e). Remarkably, the coherence length of the illumination field, i.e. the full width half maximum of $|\Gamma|$ is 1.2 μm in water. Following the factorization in Eq. (1), for thin samples, this spatially coherent white light behaves as an effective monochromatic field of angular frequency ω_0 . This concept has been reiterated recently by Wolf in the context of X-rays [20]. From the measurement of Γ , we found that this average frequency corresponds to a wavelength of 535 nm.

3. Static iSLIM

In order to demonstrate the quantitative capability of this instrument, we first image 1 micron diameter polystyrene beads immersed in water. Throughout our measurements, we used a 40X (0.75 NA) microscope objective. The images in Fig. 2 were obtained using a gray scale CCD (Zeiss AxioCam MRm). The interferogram is characterized by high-contrast, as shown in Figs. 2(a)-2(b). This is due to the fact that the CCD plane and the grating are in conjugate planes and the L1-L2 lens system is virtually dispersion-free. From the interferogram, the quantitative phase distribution is obtained via a spatial Hilbert transform, as described in more detail in Refs [9,10]. The faint rings visible around the beads may be due to slight defocusing and residual dispersion in our imaging optics. These can be removed in the future by using dispersion compensated camera lenses. An important feature of iSLIM is that it provides a much more uniform phase background than laser-based methods. We characterized this *spatial* noise signature by computing the *spatial* phase fluctuation histogram [Fig. 2(d)] of the background [area A in Fig. 2(c)]. The resulting standard deviation of the noise is 4.2 nm optical path-length. We believe that the dominant noise component can be reduced in the future, as it is most likely due to surface irregularities in the grating, rather than in the optical field distribution. The measured maximum path-length shift s for a bead of diameter d , $s = (n_1 - n_0)d$, with n_1 and n_2 the refractive index of polystyrene and water, respectively, is 240 \pm 4 nm, which is somewhat below the expected value of 256 nm ($n_1 = 1.589$, $n_0 = 1.333$). This underestimation may be due to possible slight defocusing in our image and also variability in the bead size distribution. For comparison, Figs. 2(e)-2(f) illustrate images obtained by DPM and 532 nm laser light. It can be seen that the phase shifts measured by the two methods agree very well.

4. Dynamic iSLIM

Due to its single shot operation, iSLIM is ideally suitable for dynamic measurements. Thus, the acquisition speed is only limited by the camera frame rate. In order to demonstrate the ability of iSLIM to perform dynamic measurements, we measured red blood cell (RBC) fluctuations. These nanoscale motions are a manifestation of Brownian motions in the RBC membrane and can provide access to the cell mechanical properties [21,22]. Fast and label-free mechanical information of RBCs may enable the discovery of new drugs for a number of diseases, including malaria and sickle cell anemia [23,24]. Whole blood from a healthy volunteer was smeared on a cover slide and imaged directly by our instrument for 25 seconds

at 10 frames/ s acquisition rate. Figure 3(a) shows the rendering of the RBC phase map at a particular time t

$$\phi(x, y; t) = 2\pi(n_{Hb} - n_{Pl})h(x, y; t) / \lambda_0 \quad (2)$$

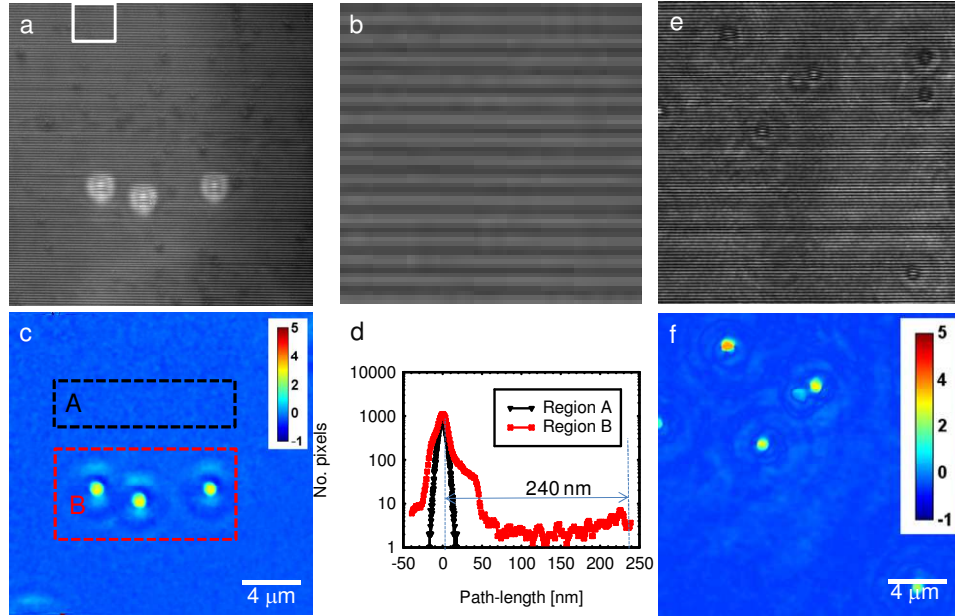


Fig. 2. a) Interferogram associated with 1 micron beads. b) Enlarged area indicated in a) that illustrates the fringe pattern more clearly. c) Reconstructed phase image for the beads in a; color bar indicates phase shift in radians. d) Histograms of the path-length distribution in the areas selected in c. e) Interferogram associate with 1 micron beads acquired with DPM [12]. f). Reconstructed phase image for the beads in e; color bar indicates phase shift in radians.

with n_{Hb} and n_{Pl} the refractive indices of hemoglobin and plasma, respectively, and h the local cell thickness. The temporal standard deviation map of the phase fluctuations was calculated as

$$\Delta\phi(x, y) = \sqrt{\overline{[\phi(x, y; t) - \overline{\phi(x, y; t)}]^2}} \quad (3)$$

where the horizontal bar indicates temporal average. The rms phase displacement map of the red blood cell is revealed in Fig. 3(b). In order to characterize the overall stability of the instrument against phase noise, we imaged an empty field of view for the same duration and at the same acquisition rate as for the RBC measurements. The histogram of the noise optical path-length fluctuation is shown in Fig. 3(c). The high signal around the cell edge and dimple is due to slight translations of the cell. It can be seen that this noise signature is essentially Gaussian, with a standard deviation of 1.3 nm. We believe that this noise level can be improved further by limiting the slight transverse vibrations of the grating, which displaces residual impurities within the field of view.

5. RGB iSLIM

An important feature of iSLIM stems from the broad spectrum of light which grants immediate potential for spectroscopic imaging. Here we demonstrate an effortless implementation of quantitative phase imaging at 3 different colors by simply recording the interferogram with an RGB camera (Zeiss AxioCam MRc). The spectral response for each of the channels is presented in Fig. 1(d). The central wavelengths for each of the red, green, and

blue channels are $\lambda_R = 620$ nm, $\lambda_G = 530$ nm, and $\lambda_B = 460$ nm. Thus, from a single RGB frame, we simultaneously reconstruct quantitative phase images at all 3 colors. We used this approach to image both beads [Fig. 4(a)-4(d)] and RBCs [Fig. 4(e)-4(h)]. The wavelength-dependent phase in this case can be written as

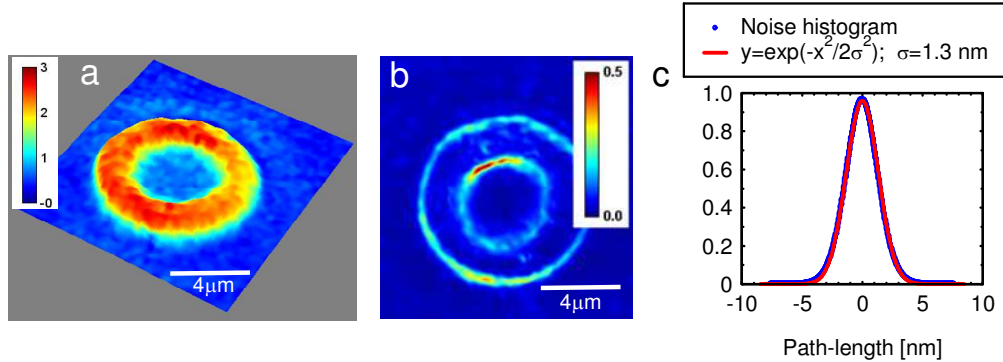


Fig. 3. a) Reconstructed phase image of a red blood cell; color bar indicates phase shift in radians. b) The r.m.s. phase displacement map of the red blood cell in a; color bar in radians. c) Histogram of the phase displacement associated with the background and the fitting with Gaussian distribution, as indicated.

$$\phi(\lambda) = \frac{2\pi}{\lambda} \Delta n(\lambda) h \quad (4)$$

where Δn is the refractive index contrast with respect to the surrounding fluid. We note that for beads [Fig. 4(d)], $\phi(\lambda) \propto 1/\lambda$, which indicates that the dispersion of polystyrene and water is small in the visible spectrum, as expected.

The similar curves associated with RBCs show qualitative differences, as exemplified by data from 3 points across the cell [Fig. 4(h)]. This result suggests that the hemoglobin and surrounding plasma may exhibit measurable dispersion in the visible spectrum, which iSLIM can quantify via a simple RGB measurement. One interesting problem to be addressed is to find out whether hemoglobin is homogeneously distributed inside the cell. The RGB measurement will provide insight into the mean cell hemoglobin concentration (MCHC), mean cellular oxygen saturation level, or even report on these parameters at subcellular scale. In particular, the MCHC is a crucial indicator for various abnormalities in the blood and, thus, is commonly assessed during blood testing. We recently found that knowledge of MCHC is necessary for accurate cell volume measurements based on phase imaging [25]. We anticipate that using the RGB information, iSLIM will gain clinical relevance, due to the combination of high throughput, via the single shot measurement, with molecular specificity from the dispersion measurement.

6. Summary and conclusions

We have developed Instantaneous Spatial Light Interference Microscopy, an add-on module that attaches to a commercial phase contrast microscope and converts it into a single-shot, common-path quantitative phase contrast microscope. With a RGB camera installed for acquisition, we obtained simultaneous phase imaging at multiple colors. In principle, any RGB camera can work for this purpose, but performance in terms of phase stability, i.e. signal to noise, may vary. iSLIM's features advance the field of quantitative phase imaging by several accounts: i) provides speckle-free images, which allows for *spatially* sensitive optical path-length measurements; ii) uses common path interferometry, which enables *temporally* sensitive optical path-length measurement; iv) due to the broad band illumination iSLIM provides phase dispersion imaging; v) and inherently multiplexes with fluorescence imaging

for multimodal, in-depth biological studies. Further the combination between the low-coherence properties of the illumination field and high numerical aperture of the microscope objective provides unique potential for single cell tomography with micron-level axial resolution. We foresee that iSLIM is likely to make a broad impact by its low-maintenance and straightforward implementation with existing phase contrast microscopes.

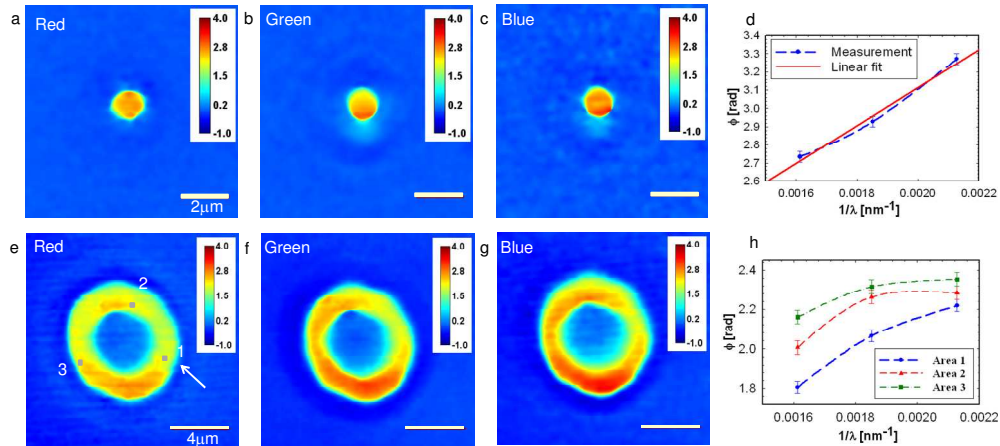


Fig. 4. RGB quantitative phase imaging for 1 micron bead a-c) and red blood cell e-g); d) the maximum bead phase values vs. wave number; h) the phases associated with the squares in e vs. wave number.

Acknowledgements

This research was supported in part by the National Science Foundation (CAREER 08-46660) and the Grainger Foundation. H. D. acknowledges helpful discussions with Zhuo Wang and Mustafa Mir. For more information, visit <http://light.ece.uiuc.edu/>.